



POLITECNICO
MILANO 1863

SCUOLA DI INGEGNERIA INDUSTRIALE
E DELL'INFORMAZIONE

EXECUTIVE SUMMARY OF THE THESIS

Baroreflex control implementation and performance evaluation of a cardiovascular hybrid mock circulation loop

LAUREA MAGISTRALE IN BIOMEDICAL ENGINEERING

Author: GUIDO EVANGELISTI, FEDERICA MECHELLI

Advisor: PROF. MARIA LAURA COSTANTINO

Co-advisor: FRANCESCO DE GAETANO, PHD

Academic year: 2021-2022

1. Introduction

Mock circulatory loops (MCL) are used to multiple purposes like training and research including the in vitro assessment of Ventricular Assist Devices (VADs) and other Cardiac Assist Devices (CADs). Usually conventional hydraulic mock loops (MCL) are used but the versatility is limited because whenever different patient conditions need to be tested, hardware changes are required. Numerical MCL instead allow for a wide reproducibility and controllability of the cardiovascular system features by means of lumped parameter modeling. The concept of merging numerical and physical models was exploited in the last years leading to a new concept of circulatory models called hybrid (H-MCL). Due to the demands for this requirements to be achieved, our thesis work has been developed. We aim at the development of a H-MCL providing realistic hemodynamic waveforms in different scenarios including rest, exercise, infarction, with and without cardiovascular device support. The mock circulatory loop we are presenting is a versatile and user-friendly set-up that is able to perform in two main configurations:

- *Baroreflex*: Patient recovery assessment including baroreflex control mechanism act-

ing on heart rate (HR), elastance (E), peripheral resistances (R_{ap} , R_{as}) and systemic venous unstressed volume (V_0).

- *Device Testing*: Cardiovascular device interaction analysis with the numerical model.

2. Materials and Method

The mock circulatory loop we are presenting is a hardware-in-the-loop system that consists in three parts: software, hardware and interface between them.

The main software part is the numerical model of the circulatory system which allows us to have physiological waveforms. The flow rate of the test blood pump is fed back into the numerical model, which will alter the pressure values. Software also contains PI controllers for pressure and level in the two tanks. The model is implemented in MATLAB Simulink, the latter is in fact a tool to solve ordinary differential equations (ODEs) and it provides a real time simulation for this test bench application. The circulation model is a lumped parameter model (LPM) of the circulatory system. Concerning the hardware, the set-up can be divided into: (1) hydraulic, (2) pneumatic and (3) electric.

2.1. Numerical Model

The main blocks of our numerical model are:

- Inputs and Process: data acquisition from level sensors, pressure sensors and flowmeter takes place here. Then the voltage signal is converted to the physical units at issue.
- Circulation Model: circulatory system model based on the work of Colacino[1].
- Level Control: PI controller to allow fluid volume balance between the two tanks. The controller compensates for unbalances by changing the speed of the backflow pump. The derivative gain (K_p) is 150, integral time (T_i) is 2, the anti-windup parameter (K_{aw}) is set as 5.
- Pressure Control: two PI controllers are used because of the need of a continuous and modulated control of the pressures in the two tanks. The controllers work on the opening areas of the proportional valves allowing the experimental tracings to follow the the numerical one. For the left ventricle, a proportional gain-scheduling control (P-scheduling) is added to improve the performance of the pressure control when the set point varies dramatically.
- Outputs: elaboration of signals to control the opening and closing of the proportional valves and the speed of the backflow pump.

2.1.1 Circulation Model

Our circulatory system model provides a real-time simulation for this test bench application. As before said, the model of the vascular network is a lumped parameter model (LPM), therefore the 3-D space distribution of the physical quantities in the system is neglected. The main blocks are:

- Left Heart: time-varying elastance model with internal resistance for both atrium and ventricle.
- Right Heart: time-varying elastance model with internal resistance for both atrium and ventricle.
- Pulmonary Circulation: described as a five element Windkessel model for the arterial system and a classic Windkessel model for the venous one.
- Systemic Circulation: the block includes a five element Windkessel model and the sys-

temic venous resistance autoregulation.

- Baroreflex: implementation of the pressure control mechanism based on the baroreceptors feedback. If the *Device testing* mode is selected in the GUI, this block acts on the venous compliance unstressed volume and peripheral resistances with reference to Colacino [1]. On the other hand, if the *Baroreflex control* mode is selected, the model is modified including heart rate control accordingly to Ursino [2].

2.1.2 Baroreflex

The baroreflex control implemented is meant to act on arterial pulmonary resistances, systemic peripheral resistances, venous unstressed volume and heart rate according to the Ursino [2] and Colacino [1] model.

The control mechanism ruling arterial systemic and pulmonary resistances can be described by a first order dynamic equation choosing $K=-0.01$ and the time constant $\tau=1$ s. Similarly, the controller of the venous compliance unstressed volume is a first order dynamic with $K=-10$ and $\tau=10$ s. The Ursino model instead replicates the baroreflex activity considering the afferent pathway, the efferent sympathetic, the parasympathetic pathways, and the response of the diverse effectors. The afferent pathway is described by a first order linear differential equation followed by a sigmoidal static function. The efferent pathways behave according to a monotonically decreasing exponential static curve for the sympathetic activity, and an analogue increasing one for the parasympathetic. The response of the effectors depends on both the activities. The generic response to the sympathetic action is comprised of a delay, a logarithmic static function and a linear first-order dynamics, whilst the response to the parasympathetic changes in the static function, which is no more logarithmic, but linear and monotonic.

2.1.3 Graphic user interface

The graphic user interface (GUI) we built makes the software more user-friendly. It will guide step by step the user and it will show pressure-volume loops and pressure tracings changes in real-time. The user can start by choosing the kind of cannulation, and then move to the se-

lection of the type of test to run, by clicking either the *Device testing* or the *Baroreflex control* mode. An example of left cannulation GUI is provided in Figure 1. The two sliders at the bottom of the window are inserted in order to change HR and CF during the simulation, without having to act directly on the code. Concerning the right cannulation choice instead, because of the fact that right heart failure is usually a result of left ventricular failure, three sliders appear, giving the user the possibility to change HR, CF_{LV} and CF_{RV}

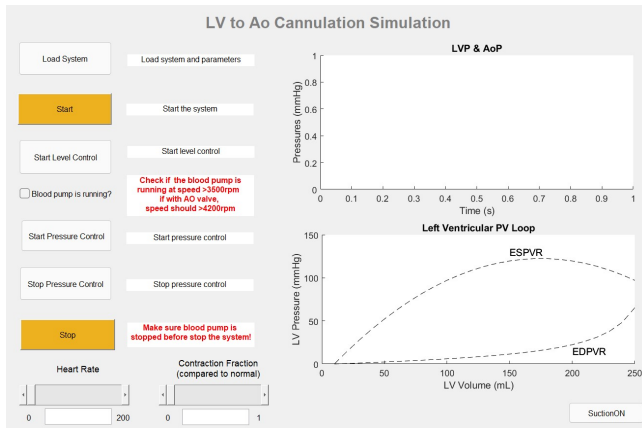


Figure 1: GUI in left cannulation VAD testing mode.

2.2. Hardware

The hardware is composed of hydraulic, pneumatic and electric circuits that work at once and intertwine to recreate the physiological pressure waveforms.

2.2.1 Hydraulic and Pneumatic

The hydraulic part is mainly composed of two cylindrical PMMA tanks ($h=164$ mm, $\phi=150$ mm). The tanks can be any anatomic district of interest. In our case, we use a numerical model of the CVS and for that reason the two chambers are meant to be the left ventricle (LV) and the aorta (Ao), if the left cannulation is chosen, or right ventricle (RV) and pulmonary artery (PA) in case of right cannulation choice. The actuators are six proportional solenoid valves (PVQ33-5G-23-01F, SMC, Japan): two inlet valves are connected to the compressed air regulator to let the compressed air come into the tanks, while the others four outlet valves are connected to a vacuum chamber to let the air go

out of the tanks. Compressed air passes through a filter regulator (LFR-1/4-D-MIDI-40um, Festo, Germany), then it is split in two routes owing to other two regulators (AR30, SMC, Japan). In the first line air with 0.4 MPa is provided to a vacuum ejector (ZL112-K15LOUT-E26L-Q, SMC, Japan), which generates a vacuum pressure that rounds -80kPa inside a vacuum chamber, and then to the two inlet solenoid valves. The second line goes directly to the four outlet valves placed on the top surface of the tanks. A schematic is proposed in Figure 2.

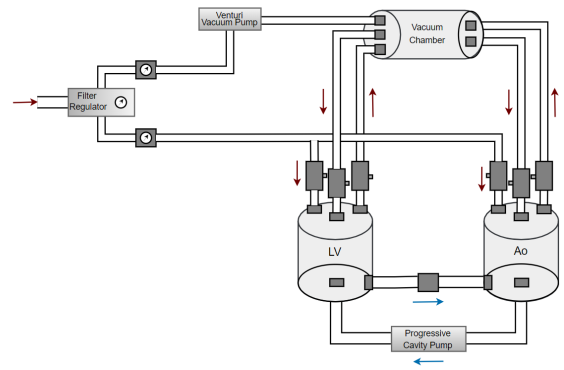


Figure 2: Main hydraulic and pneumatic schematic components.

The backflow pump is a self-priming volumetric progressive cavity pump (MAE25-1, CSF Inox, Italy) which adjusts the fluid level in the chambers. A relay (JQC-3FF-S-Z) has been installed for safety in case of an excessive increase of the left ventricle tank level. In that case, the relay will switch automatically the rotation direction from clockwise to counter-clockwise up to when the LV water level reaches a safe value.

2.2.2 Electric

Because of the presence of several kinds of actuators and sensors, different supplies of energy are required. That source of energy is provided by one power supply (SDR-240, Mean Well, Taiwan) that can yield 24VDC and another one (DPP480-48-1, TDK-LAMBDA, Japan) that provides 48VDC. To provide pressure and level measurements for feedback, two pressure sensors (PN2069, IFM Electronic, Germany) are installed on the bottom of the two tanks while an infrared range finder (GP2Y0A41SK0F, Sharp, Japan) is placed on the top surface of the chambers. The level sensors requires 5VDC and so a

linear voltage regulator (L7805ACV, ST Microelectronics, Switzerland) is used to convert and stabilize the 24VDC energy source.

The communication between hardware and software parts is achieved using a DAQ card (MF634, HUMUSOFT, Czech Republic) as interface: its role consists in sensor data acquisition and communication to the model. After the model is fed, it will trigger the actuators, which are comprised of proportional valves and the backflow pump.

2.3. Test Protocol

The first validation deals with the numerical model. In particular, we want to assess the validity of the numerical model in:

- response in real-time HR and CF changes made by user using the sliders in the GUI during the simulation.
- replication of different patients' conditions varying pressure tracings consistently with the input parameters chosen by the user.
- restoring almost-physiological waveforms when baroreflex control is active.

Once the numerical model has been validated, we move to the comparison between numerical tracings and experimental ones. The two main curves we computed are pressure tracings over time and PV loops. The accuracy in the experimental measures has been evaluated considering two functional indexes:

- pressure error

$$err = \frac{\sum |P(t)_{exp} - P(t)_{num}|}{t_{simulation}} \Delta t \quad (1)$$

- stroke work

$$SW = \oint P_{LV} dV \quad (2)$$

The last tests deals with the introduction of a ventricular assist device in the mock loop in order to assess its interactions with the numerical cardiovascular model of the patient.

3. Results

3.1. Numerical Model Validation

The first section of our tests seeks to validate the numerical model flexibility by changing HR and CF in real-time, looking at pressure tracings and PV loop variations. In Figure 3 numerical

pressure variations are reported. The HR starts at 120 bpm, then it is switched to 80 bpm, and then again at 40 bpm. The CF is fixed to 1.

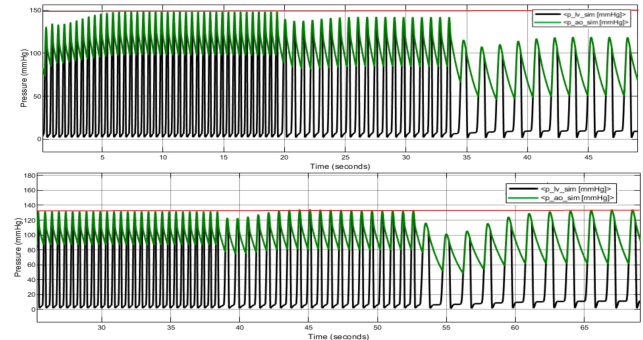


Figure 3: Ventricular and aortic numerical tracings varying HR. In the upper panel no baroreflex is implemented, the re-adjustment does not occur. In the lower panel the baroreflex control is implemented for the UVV and the SVR: ventricular pressure tracings readjust to almost physiological HR after a few heart cycles (red line).

The same analysis is performed maintaining HR=60 bpm and changing CF from the starting value 1 to 0.5 and then to 0.2 (Figure 4).

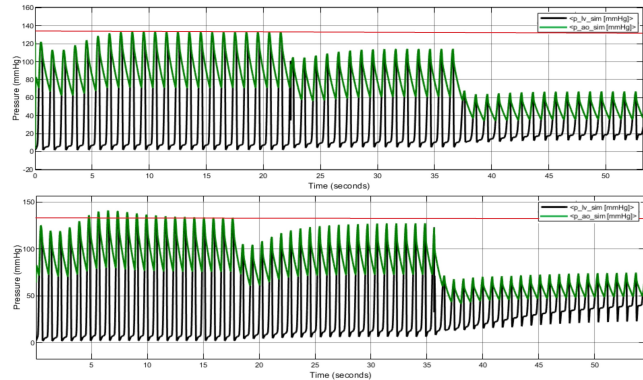


Figure 4: Ventricular and aortic numerical tracings varying CF. When baroreflex is not active (upper figure) tracings peaks always lower when CF decreases. In the lower panel the baroreflex controls the UVV and the SVR: ventricular pressure tracings readjust to almost physiological pressures (red line), except for the case CF=0.2 because ventricular residual contraction is too small.

In Figure 7 the mock loop response in reproducing PV loops is assessed by changing the HR

(upper figure) or the CF (lower figure).

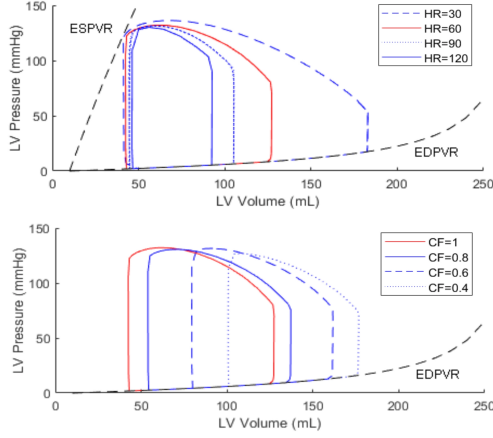


Figure 5: PV loop variations considering HR variability (upper figure) and CF variability (lower figure).

The parameters that can be changed directly in the numerical model to represent different clinical conditions are a multitude. In this framework, just as an example of the adaptability of the model, we decide to vary the aortic resistance so as to mimic a stenotic heart valve and to see how pressures and flow rates adapt. Using constant HR and CF, we compare two different conditions: (1) $R_{valve}=0.00375$ mmHg · s/ml (2) $R_{valve}=0.08$ mmHg · s/ml. Increasing the valve resistance in the numerical model causes the numerical the flow rate through the simulated valve to decrease.

At last, we wanted to end the baroreflex model assessment by looking at heart rate (HR) and systemic arterial resistance (R_{sa}) variations by acting directly on the aortic pressure:

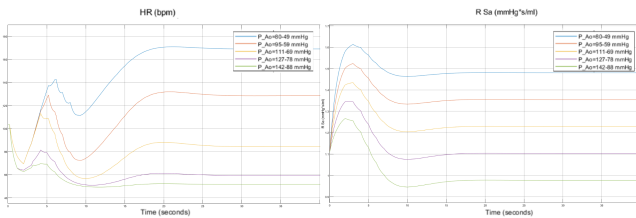


Figure 6: HR and R_{sa} variation: systemic vascular resistances and HR both decrease when blood pressure increase is detected.

3.2. Experimental and Numerical Tracings Comparison: Pressure Waveforms and PV Loops

Once the numerical model has been validated, experimental and numerical tracings have been compared. The pressure control is supposed to follow the numerical tracing, minimizing the average error, and to trigger the electrovalves opening and closure consistently. The results about left and right cannulation in physiological conditions (CF=1, HR=60) are reported:

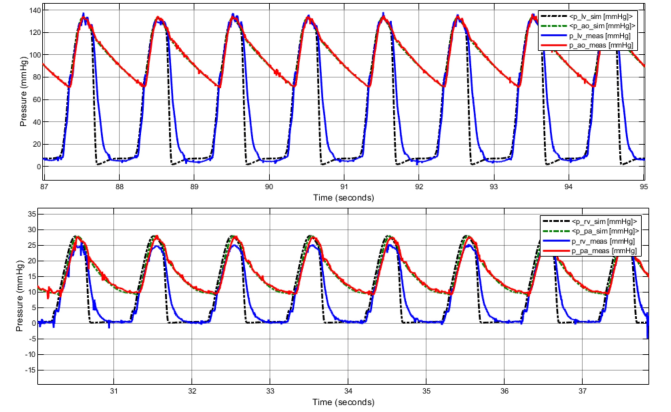


Figure 7: Experimental pressure tracings following the numerical ones. Left ventricular and aortic pressure in the upper figure. Right ventricular and pulmonary artery pressure in the lower panel.

In Figure 8 the CF parameter is varied and the RV-PV loop is analysed. Even though the PV loops don't completely overlap, by analysing the SW of the numerical and the experimental PV loops at different CF, we see that they decrease by very similar ΔSW using the equation:

$$\Delta SW_{CF} = \frac{|SW_{CF_i - \Delta_i} - SW_{CF_i}|}{SW_{CF_i}} \cdot 100\% \quad (3)$$

Table 1: Numerical and experimental ΔSW calculations (Equation3) at different CF.

	Num ΔSW_{CF}	Exp ΔSW_{CF}
$\Delta SW_{CF=1/CF=0.8}$	2.07%	2.7%
$\Delta SW_{CF=0.8/CF=0.6}$	13.02%	13.64%
$\Delta SW_{CF=0.6/CF=0.5}$	20.4%	22.04%
$\Delta SW_{CF=1/CF=0.6}$	14.82%	15.97%
$\Delta SW_{CF=1/CF=0.5}$	32.18%	34.49%

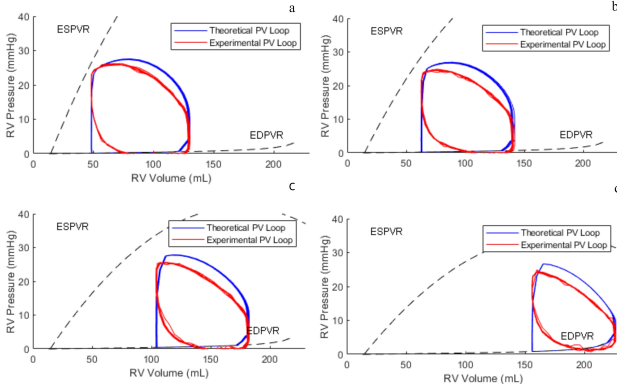


Figure 8: Numerical and experimental PV loops for the RV at HR=60 bpm and a) CF=1, b) CF=0.8, c) CF=0.6, d) CF=0.5.

3.3. VAD Integration

In order to assess the VAD-patient cardiovascular model interactions we used a continuous centrifugal pump, which can be seen as an analogue of a centrifugal flow VAD as far as its functioning is concerned. The flow probe (H9XL, Transonic Systems Inc, USA) is placed downstream the pump. In Figure 9 pressure tracings and PV loops at two different assistance levels ($q_{bp}=2.1$ l/min and $q_{bp}=4$ l/min) are shown. Pathological conditions (HR= 90 bpm and CF=0.34) are chosen for the left ventricle. When the elaborated flow rate increases, the PV loop shifts leftwards (i.e. the LV volume decreases). The experimental PV loop superposes to the theoretical one, except for the last part of the isovolumic relaxation and the beginning of the diastolic filling. P_{Ao} tracing tends towards a straight line with higher flow rates, while the P_{LV} tracings slightly shift to lower pressures, with peaks going from about 110 mmHg to about 95 mmHg and valleys

from 20 mmHg to 5 mmHg.

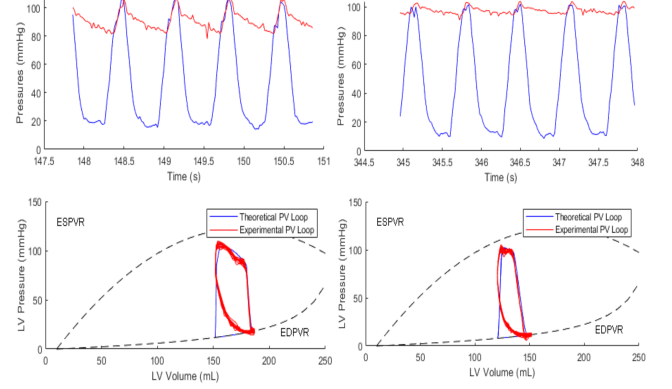


Figure 9: Pressure and PV loop tracings for the LV with vad assistance at a) $q_{bp}=2.1$ l/min, b) $q_{bp}=4$ l/min.

4. Conclusions

The slider control allows the user to easily change HR and CF and we can see the influence of these two parameters when the control of the baroreceptor is completely deactivated. When the baroreflex control is activated instead, the model we implement is capable of restoring a quasi-complete physiological pressure tracing (if the myocardium is not severely impaired) a few cycles after the real-time modifications of HR and CF.

Pressure-volume loop analysis gives additional worth to the numerical model. Increasing the HR, the end-diastolic volume reduces, leading to a reduction of the SW. Varying the CF from healthy to pathological, SW decreases with the reduction of contractility causing reduced ejection, lower blood pressure, higher end-systolic volume and as a consequence reduced ventricular filling.

The flexibility of our mock loop has been checked changing the aortic valve resistance in the numerical model. Several parameters can be changed and monitored, and in our experiment the aortic resistance variation was taken into consideration as an example. As we expected, an increase in the valve resistance leads to higher ventricular pressure and lower flow rate through the aortic valve in the numerical model. Concerning the baroreflex results reported in Figure 6 we find accordance with the literature [3]. The two main actions of the baroreflex feedback are: (1) pressure buffering and (2) cardio-protection. We see that our model decreases systemic vascu-

lar resistances when blood pressure rises in order to buffer pressure and that it decreases HR (rising the parasympathetic tone and decreasing the sympathetic one), for cardio-protection.

The comparison between experimental and theoretical pressure shows that the controller is capable of making the experimental pressure waveforms follow the numerical tracings, especially at low frequencies. Increasing the frequency, the pressure error increase too, it is mainly due to: (1) need for controller parameter optimization, (2) mechanical components inertia, (3) instability of compressed-air line. These differences between the experimental and the numerical tracings are evident also in the PV loop analysis, in particular the LV PV loop is not able to completely follow the isovolumic relaxation. The RV PV loop main errors are instead in the ventricular ejection, and they are due to the PI controller parameters.

When integrating the continuous centrifugal pump, we can appreciate what happens with different levels of assistance. Figure 9 shows how PV loops shift towards lower LV volumes and that the P_{Ao} curve flattens. That is due to the fact that, the more the VAD works, the more the flow rate will not rely on the heart, and the less it will display the pulsatility that the pump doesn't produce. Being a constant flow in time, the pressure getting in the aorta will be constant in time as well.

References

- [1] Francesco M Colacino, Francesco Moscato, Fabio Piedimonte, Maurizio Arabia, and Guido A Danieli. Left ventricle load impedance control by apical vad can help heart recovery and patient perfusion: a numerical study. *Asaio Journal*, 53(3):263–277, 2007.
- [2] Mauro Ursino. Interaction between carotid baroregulation and the pulsating heart: a mathematical model. *American Journal of Physiology-Heart and Circulatory Physiology*, 275(5):H1733–H1747, 1998.
- [3] So-Hyun Jansen-Park, Mohammad Nauzef Mahmood, Indra Müller, Lisa Kathrin Turnhoff, Thomas Schmitz-Rode, Ulrich Steinseifer, and Simon Johannes Sonntag. Effects of interaction between ventricular assist de-

vice assistance and autoregulated mock circulation including frank–starling mechanism and baroreflex. *Artificial organs*, 40(10):981–991, 2016.